Wind and Structures, *Vol. 25, No. 4 (2017) 397-413*
DOI: https://doi.org/10.12989/was.2017.25.4.397

Ground effects on wind-induced responses of a closed box girder

Wenhao Mao[1,2] and Zhiyong Zhou[*1]

[1]*State Key Laboratory for Disaster Reduction in Civil Engineering, 1239 Siping Road, Shanghai, China*
[2]*Key Laboratory of Ministry of Communications for Bridge Structure Wind resistance, 1239 Siping Road, Shanghai, China*

(Received June 21, 2017, Revised September 27, 2017, Accepted September 28, 2017)

Abstract. When bridges are constructed with lower heights from the ground, the formed channel between the deck and the ground will inevitably hinder or accelerate the air flow. This in turn will have an impact on the aerodynamic forces on the deck, which may result in unexpected wind-induced responses of bridges. This phenomenon can be referred to "ground effects." So far, no systematic studies into ground effects on the wind-induced responses of closed box girders have been performed. In this paper, wind tunnel tests have been adopted to study the ground effects on the aerodynamic force coefficients and the wind-induced responses of a closed box girder. In correlation with the heights from the ground in two ground roughness, the aerodynamic force coefficients, the Strouhal number (S_t), the vortex-induced vibration (VIV) lock-in phenomena over a range of wind velocities, the VIV maximum amplitudes, the system torsional damping ratio, the flutter derivatives, the critical flutter wind speeds and their variation laws correlated with the heights from the ground of a closed box girder have been presented through wind tunnel tests. The outcomes show that the ground effects make the vortex-induced phenomena occur in advance and adversely affect the flutter stability.

Keywords: ground effects; wind tunnel test; closed box girder; aerodynamic force coefficients; S_t number; VIV; critical flutter wind speeds

1. Introduction

Among the wind-induced vibrations, flutter is a self-excited aerodynamic instability phenomenon. Once flutter occurs, the amplitude keeps increasing, resulting in serious harm such as the collapse of old American Tacoma Bridge in 1940 (Larsen 2000). Therefore, in the modern bridge wind-resistant design, flutter stability is the primary goal. Although the vortex-induced vibration is a limited amplitude response, it is prone to occur at low wind speeds with relative large amplitude, which will affect the traffic safety, the strength and fatigue resistance of the structure and may even induce other types of instability such as cable vibrations. Thus, in modern wind-resistant design for bridges, VIV performance design is also raised to an important position.

Nowadays, many existing and under-construction bridges, such as Shenzhen-Hong Kong Channel Bridge, are built with lower heights from the ground. Additionally, for those bridges

*Corresponding author, Professor, E-mail: z.zhou@tongji.edu.cn

http://www.techno-press.org/?journal=was&subpage=7 ISSN: 1226-6116 (Print), 1598-6225 (Online)

located above the reservoir, with the rise of water level, the deck comes closer to the water surface. In these cases, the air flow around the bridge girders, as a result of interactions with the ground or water surface, is definitely different from the conventional cases of bridges at a certain height. This phenomenon can be regarded as "ground effects".

So far, research into ground effects on the wind-induced responses of closed box girders has not been performed by scholars. Normally, the studies of ground effects at home and abroad are mainly concentrated on the aerospace engineering, where most of the researches applied experimental approaches (Justin *et al*. 2012, Yang *et al*. 2015, Marshall *et al*. 2010, Yang and Yang 2014) and numerical simulations methods (Mokry 2001, Barber 2006, Park and Lee 2008, Prasad 2014, Lee *et al*. 2010, Mahon and Zhang 2005) to study the ground influences on the wings. Justin *et al*. (2012) adopted experimental methods to study ground effects on NACA4412 airfoil under different wind attack angles and low Reynolds numbers respectively. Yang *et al*. (2015) used the mobile road simulation systems and six-component balance measuring system in wind tunnel tests to study the ground viscous effects on aerodynamic characteristics of the wing in ground (WIG).

Marshall *et al*. (2010) and Yang and Yang (2014) studied the influence of boundary layer effects on the ground effects by wind tunnel test method and the results showed that the thickness of the boundary layer reduced the effective height in WIG wind tunnel tests so that ground effects became stronger. Mokry (2001) adopted numerical simulation methods to study the ground effects on dissipation and movement of the trailing vortex of the aircraft. Studies showed that the ground effects accelerated the vortex dissipation. Barber (2006) used experimental and numerical simulation methods to study the ground effects on aerodynamic responses of the structure. Park and Lee (2008) adopted numerical simulation methods to study the ground effects on static and dynamic stability of the wing endplates and explained the reasons for the variation of lift coefficients. The results showed that the ground effects decreased the aerodynamic stability of the wing endplates. Prasad (2014) applied numerical simulation methods to study the water wave effects on the wing. Lee *et al*. (2010) studied the influence of wing configurations on aerodynamic characteristics by numerical simulation methods.

Scholars have conducted many researches into bridge VIV (Diana *et al*. 2010, Sarwar and Ishihara 2010, Wu and Kareem 2013, Williamson and Govardhan 2004, Zhou *et al*. 2015) and flutter stability (Chen and Zhou 2006, Matsumoto *et al*. 1999, Yang and Ge 2009), but no systematic studies on bridge VIV and bridge flutter stability considering the ground effects have been performed. It can be expected that the "channel" between the deck and the ground will hinder or accelerate the air flow. This in turn will affect the aerodynamic forces on the deck, which will have an impact on the aerodynamic force coefficients, the flutter stability and the vortex-induced vibrations of the bridges.

In this paper, wind tunnel tests have been adopted to study ground effects mechanism on the aerodynamic force coefficients, the vortex-induced vibrations and the flutter stability of a closed girder. First, the variation laws of the aerodynamic force coefficients and the S_t number correlated with the height from the ground have been studied. Second, the VIV lock-in phenomena over a range of wind velocities, the maximum amplitudes and the variation laws correlated with the height have been determined through wind tunnel tests. At last, the system torsional damping ratios, the flutter derivatives, the critical flutter wind speeds and their variation laws correlated with the height from the ground of the closed box girder have been presented through wind tunnel tests.

2. Experimental details

2.1 Section model design

A section model with high rigidity is required in the force measurement and vibration measurement wind tunnel tests. In this study, the model had a length L of 1.2 m, a height h of 0.047 m, and a width B of 0.3647 m, with the length-width ratio of 3.3. The scale ratio is 1 : 85.

The design of the model is shown in Fig. 1, where railings were installed only in the VIV tests. Height H from the ground was defined in Fig. 2. Particularly, the height H from the ground refered to the distance from the bottom surface of the model to the ground (uniform flow field) or the rough strip top surface (turbulent flow field). Rough strip layout and the position of section model in turbulent flow field were shown in Fig. 3. The side length d of each rough strip was 0.05 B and the size of each rough strip was 0.018 × 0.018 × 2.4 m. Up to 24 rough strips were arranged here, with a centre distance of 0.108m and a clear spacing of 0.9 m, equal to 5 d.

The wind tunnel tests were carried out in the TJ-2 wind tunnel in Tongji University. In the experiments, two different ground conditions, ground with and without rough strips, were created to simulate the turbulent flow field and uniform flow field respectively.

For the force measurement tests, thirteen wind attack angles from -6° to +6° and six different heights from the ground were considered in both flow fields (see Table 1). The vibration measurement tests were conducted under three different wind attack angles, +3°, 0°, -3°, and four different heights from the ground in both flow fields (see Table 2). The free vibration method was adopted to measure the VIV lock-in ranges, the maximum amplitudes and the critical flutter wind speeds. Another free vibration method with an initial displacement was then applied to obtain the system torsional damping ratio and the flutter derivatives in two conditions.

For the force measurement wind tunnel tests, the model was set vertically on the force balance, which is shown in Fig. 4. For the vibration measurement wind tunnel tests, rigid section model was elastically suspended on the bracket in the wind tunnel through eight springs. A section model installation diagram is shown in Figs. 5 and 6.

The desired vertical frequency and torsional frequency of the whole system were achieved by determining appropriate mass and mass inertia of the entire system and adjusting the spring stiffness and spacing. Inflow speed was measured by a pilot tube and micro-manometer located in front of the model.

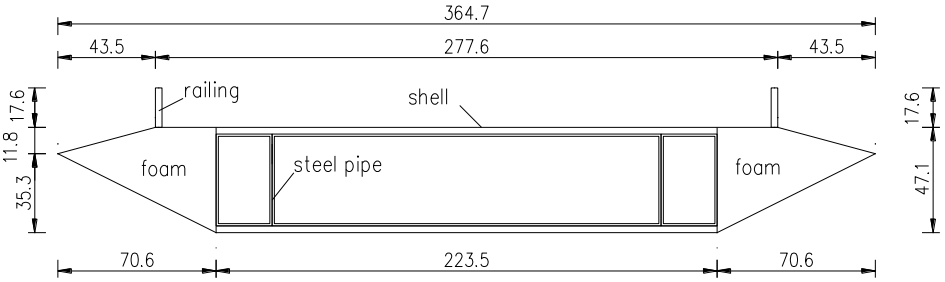

Fig. 1 Section model for VIV（unit: mm）

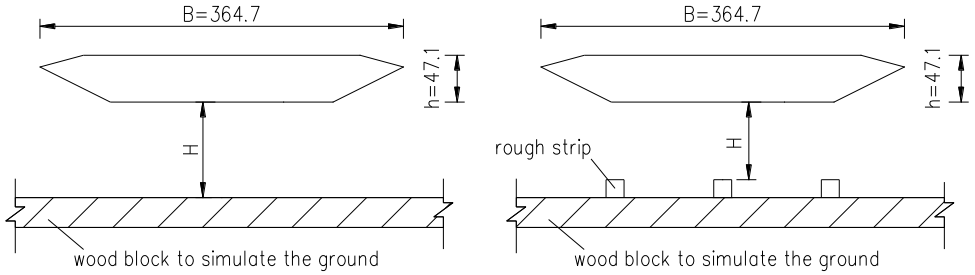

Fig. 2 Model height from the ground（unit: mm）

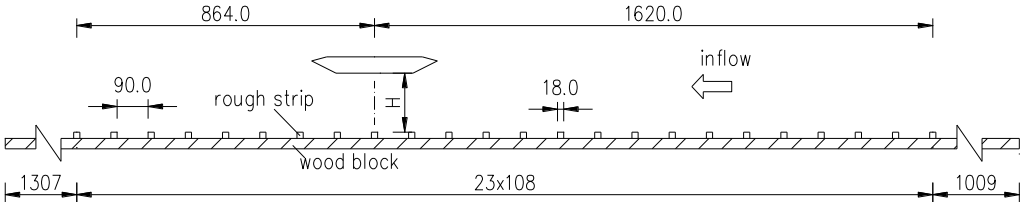

Fig. 3 Wind direction and location model（unit: mm）

(a) Without ground effects (b) Uniform flow field (c) Turbulent flow field

Fig. 4 Photos of section model force measurement tests

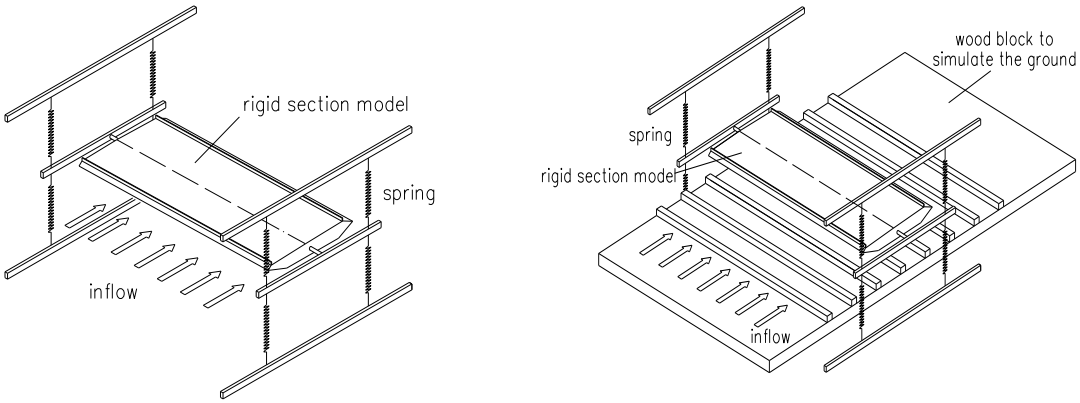

(a) Without ground effects (b) With ground effects

Fig. 5 Sketch of experimental installation

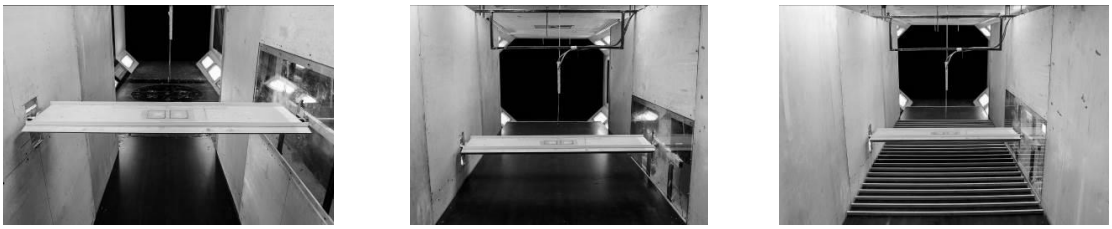

(a) Without ground effects (b) Uniform flow field (c) Turbulent flow field

Fig. 6 Photos of section model VIV and flutter measurement tests

Table 1 Cases of section model force measurement tests

Width B（mm）	Height from the ground H（mm）	H/B	Wind speed（m/s）	uniform flow field
				Attack angle
364.7	72.9	0.2	15	-6°, -5°, -4°, -3°, -2°, -1°, 0°, 1°, 2°, 3°, 4°, 5°, 6°
	109.4	0.3		
	145.9	0.4		
	182.4	0.5		
	218.8	0.6		
	1458.8	4		

Table 2 Cases of section model wind-induced vibration measurement tests

Width B（mm）	Height from the ground H（mm）	H/B	uniform flow field	turbulent flow field
			Attack angle	Attack angle
364.7	72.9	0.2	-3°, 0°，+3°	-3°, 0°，+3°
	145.9	0.4		
	218.8	0.6		
	1458.8	4		

VIV and the flutter stability are closely related to the damping ratio of the system. For this reason, before performing wind tunnel tests, the damping ratio of the system had been measured, as shown in Table 3. As VIV is likely to occur at low wind speeds, a set of springs with higher rigidity was selected in order to improve the vertical frequency of the section model system. Since this study mainly concentrated on vertical VIV, it was necessary to ensure that the torsional frequency was far away from the vertical frequency so that the mutual influence between vertical VIV and torsional VIV could be avoided. Major parameters of VIV and flutter sectional model wind tunnel tests are shown in Table 3.

Table 3 Major parameters of VIV and flutter sectional model wind tunnel tests

	Parameters of VIV section model	Parameters of flutter section model
Length $L(m)$	1.20	1.20
Height of model $h(m)$	0.047	0.047
Width $B(m)$	0.3647	0.3647
Mass per length $m(kg/m)$	5.036	3.9942
Vertical frequency $f_h(Hz)$	8.10	2.4194
Mass moment per length I_m （kg·m^2/m）	-	0.0649
Torsional frequency $f_a(Hz)$	-	4.9539
Vertical damping ratio ξ_h	4.8‰	4.8‰
Torsional damping ratio ξ_a	-	4.2‰

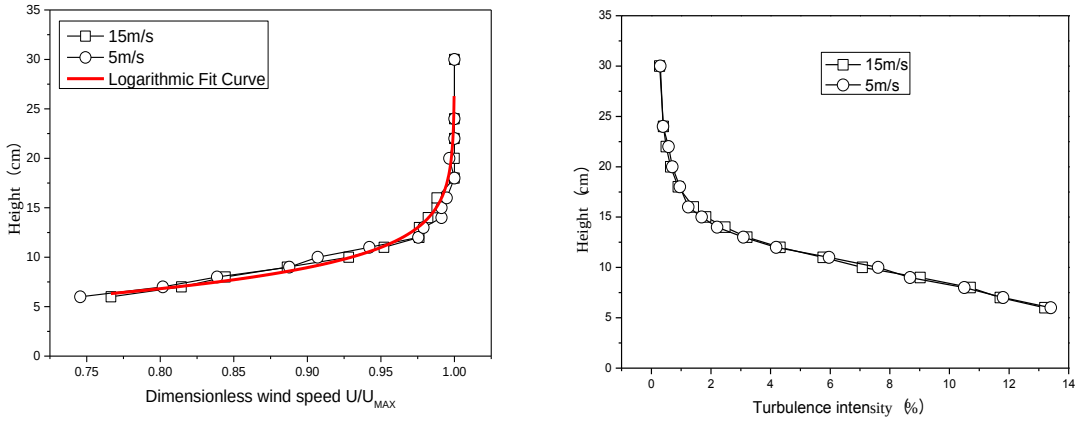

(a) Wind field profile (b) Turbulence intensity profile

Fig. 7 The average wind profiles and turbulence profile test results

2.2 Turbulence wind field profile and turbulence intensity profile test

Before the force measurement and vibration measurement tests, it was essential to achieve a stable turbulent flow field. Therefore, with the absence of the section model, 16 measuring points at different heights from the ground (the distance from measuring point to the top of rough strips were 6 cm, 7 cm, 8 cm, 9 cm, 10 cm, 11 cm, 12 cm, 13cm, 14 cm, 15 cm, 16 cm, 18 cm, 20 cm, 22 cm, 24 cm and 30 cm, respectively,) were vertically arranged in a row along the centric position of the section model. The reference wind speeds were monitored and measured with a pilot tube and micro-pressure gauge. Wind speed and turbulence data acquisition were collected by a Cobra dimensional fluctuating wind speed measuring instrument.

Fig. 7 presents the results of wind profiles and turbulence intensity profiles for the two inflow speeds of 5 m/s and 15 m/s in the turbulent flow field, which can be considered capable of

providing stable wind field profiles for the subsequent wind tunnel tests. Although this turbulent profile does not represent a boundary layer profile, the wind field profile meets very well with the Logarithmic Fit Curve, which is similar to that of the boundary layer (JTG/T D60-01-2004). In addition, the turbulence intensity profile has the same variation law with the boundary layer. Therefore, studying the ground effects on a closed box girder in this turbulence flow filed can offer a reference for relevant researches.

It could be inferred from the results that the arrangement of rough strips formed a certain thickness of the wind profile and turbulence intensity profile. The height of the profile was about 15-20 cm, which was equivalent to the height from the ground H= (0.4~0.5) B.

3. Ground effects on the aerodynamic force coefficient

3.1 The definition of aerodynamic force coefficient

Aerodynamic force coefficients refer to a dimensionless coefficient characterizing aerodynamic force on the deck under the average wind action, which reflects the unsteady aerodynamic wind effects on the bridge. This is a key parameter used to determine static response and dynamic response of the structure under wind loads. According to the body axis coordinate system of the bridge section itself and the wind axis coordinate system respectively, effects of wind on structures can be decomposed into three types of forces: aerodynamic force in wind axis are noted as drag F_D, lift F_L and moment M_T, as shown in Fig. 8.

Drag coefficient C_D, lift coefficient C_L and moment coefficient C_M are defined as follows

$$C_D = \frac{F_D}{1/2\rho U^2 HL} \quad C_L = \frac{F_L}{1/2\rho U^2 BL} \quad C_M = \frac{M_T}{1/2\rho U^2 B^2 L} \tag{1}$$

where, ρ represents the air density, ρ=1.225 kg/m^3; U represents the wind speed; H, B and L represent projection of section model height, width and length separately, α indicates the wind attack angle.

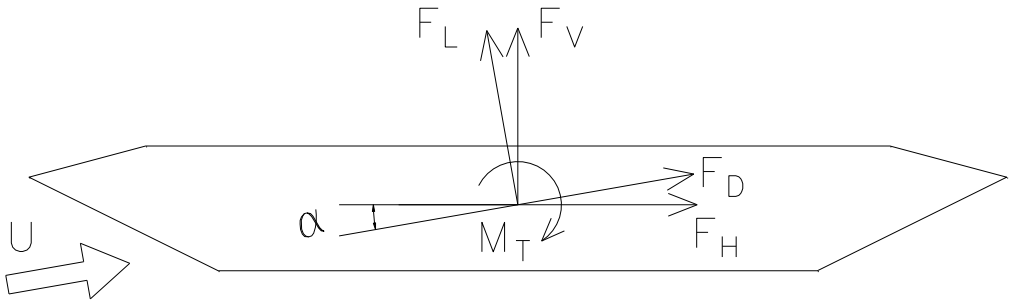

Fig. 8 Three-components of aerodynamic force diagram

3.2 Analysis of test results

Figs. 9-11 show the aerodynamic force coefficient variation curves concerning the heights from the ground both in uniform flow field and turbulent flow field. Generally, ground effects on the lift coefficients and moment coefficients are essentially unchanged, while the drag coefficients are affected more obviously. Larger wind attack angles are more likely to cause greater ground effects. In the uniform flow field, the overall trend is that the drag coefficient decreases while the height from the ground increases. This indicates that when the surface roughness is small, the closer the deck is to the ground, the greater forces will be exerted on the deck, thus will adversely affect the structure. In the turbulent flow field, although the drag coefficient grows as the height rises, drag coefficients are still larger than that in the case H/B=4.0 when H/B≥0.4. Therefore, ground effects will have a negative influence on the structure.

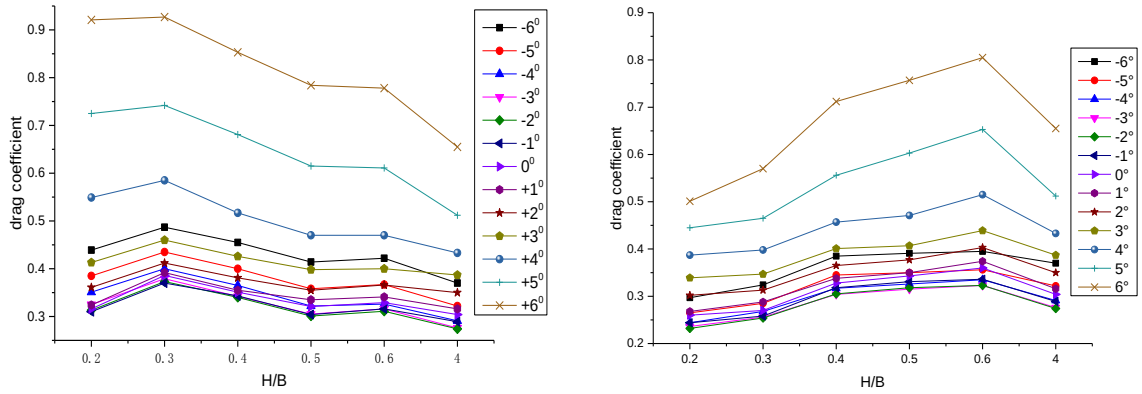

(a) Uniform flow field (b) Turbulent flow field

Fig. 9 Drag coefficient

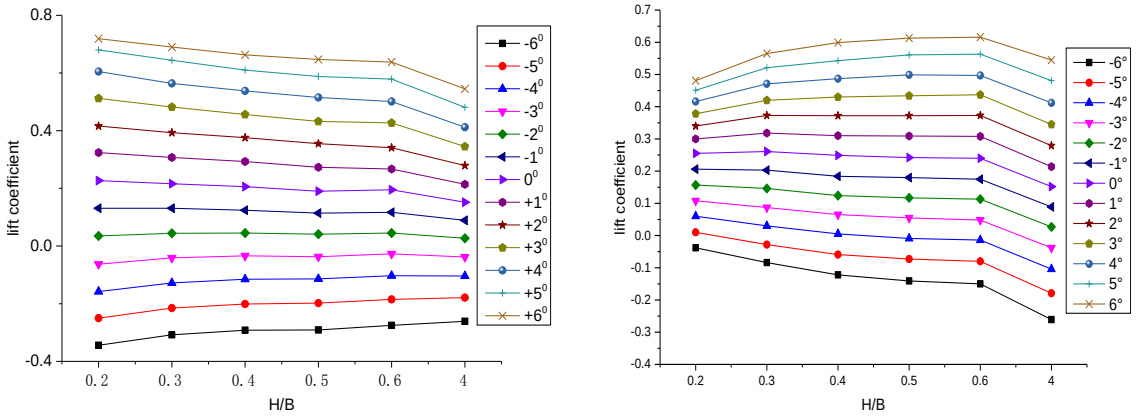

(a) Uniform flow field (b) Turbulent flow field

Fig. 10 Lift coefficient

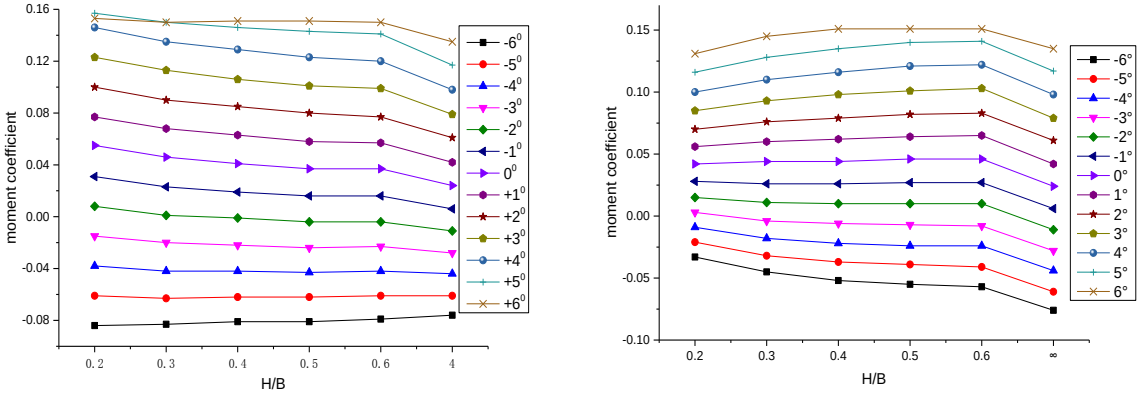

(a) Uniform flow field (b) Turbulent flow field

Fig. 11 Moment coefficient

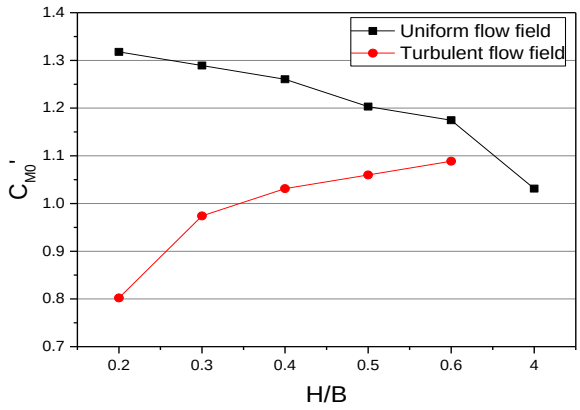

Fig. 12 The first derivative C'$_{M0}$ of the moment coefficients

3.3 Ground effects on the aerostatic stability

The aerodynamic force coefficients can be used to calculate the torsional divergence critical wind speed. According to formula (6.1.2-2) in "Wind-resistent Design Specification for Highway Bridges" (JTG / T D60-01-2004), the torsional divergence critical wind speed is

$$V_{\mathrm{td}} = \sqrt{\frac{2K_{\mathrm{t}}}{\rho B^2 C'_{M0}}} \tag{2}$$

As Eq. (2) shows, greater C'_{M0} leads to lower critical wind speed. Fig. 12 shows the experimental values of the first derivative C'_{M0} of the moment coefficients with respect to the height from ground at wind attack angle of 0°. Evidently, in uniform flow field, the value of C'_{M0} increases as the height from ground decreases, and the maximum change rate can reach

approximately 30%. This means that the aerostatic stability will largely decrease when the deck gets closer to the ground with relatively small roughness. While in the turbulent flow field, the variation law of C'_{M0} shows an opposite trend. Interestingly, when H/B is above 0.4, the values of C'_{M0} are still higher than those in the case H/B = 4.0 (in uniform flow field). This means that under turbulent flow field, the aerostatic stability will firstly decrease and then increase as the height from the ground decreases. In conclusion, ground effects can adversely affect the structural aerostatic stability. The impact of ground effects on the structural aerostatic stability should be fully considered, especially when the bridge is located above the reservoir.

3.4 Ground effects on VIV lock-in intervals

For VIV, S_t number is a dimensionless coefficient reflecting shedding frequencies of the vortex. From the formula $S_t = fD/U$, we can find that when the wind speed is at a certain value, a larger S_t number means a higher frequency of vortex shedding.

Take the case of 0° wind attack angle as representation, the S_t number variation curve is shown in Fig. 13, where f is the vortex shedding frequency, D is the section height, 0.047m, and U is the wind velocity, set as 5m/s. Fig. 13 reveals that under the constant wind speed in the uniform flow field, when the height from the ground decreases, S_t number grows and, as mentioned above, the vortex shedding frequency becomes larger.

For a specific section, normally the oscillating frequency of a certain VIV is constant. Here we can see the formula $S_t = fD/U$ again. When the f and D are constant, a higher S_t means a lower wind speed U. In other words, lower height from the ground can lead to higher S_t numbers, which results in lower wind speed. This makes vortex shedding frequency meet the oscillating frequency and finally VIV occurs. In conclusion, ground effects will impel vortex-induced vibrations to occur earlier.

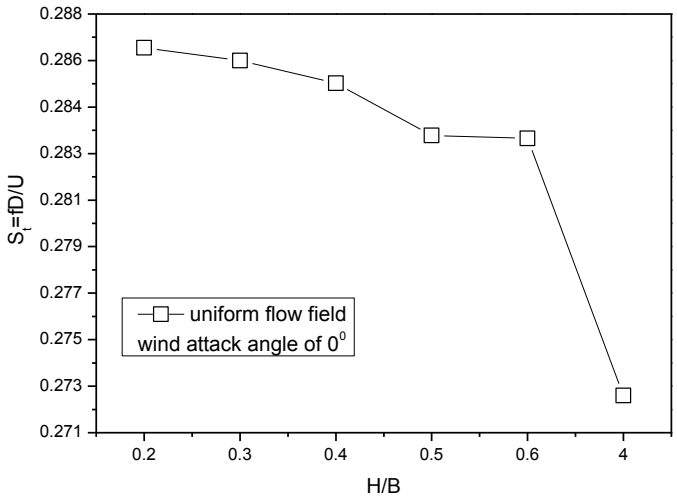

Fig. 13 S_t number test values

4. Ground effects on VIV lock-in range and amplitudes

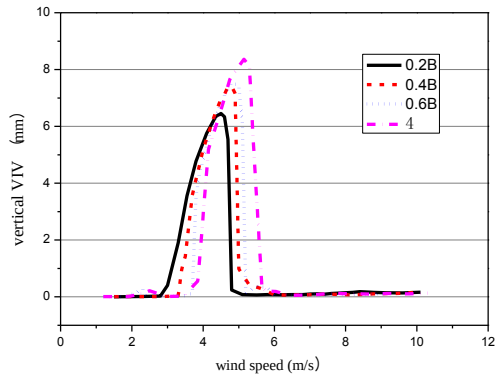

(a) uniform flow field，+3° wind attack angle

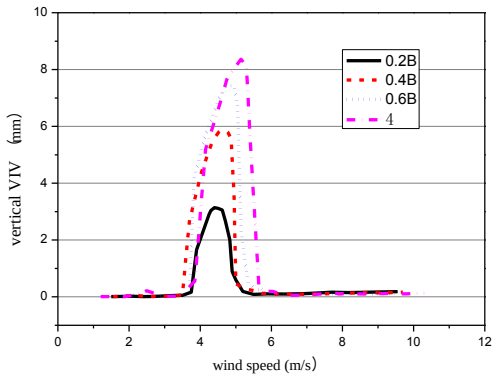

(b) turbulent flow field, +3° wind attack angle

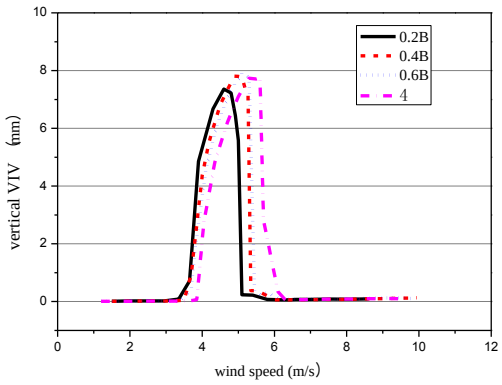

(c) uniform flow field, 0° wind attack angle

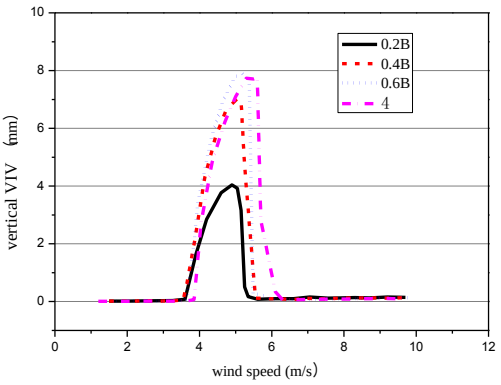

(d) turbulent flow field, 0° wind attack angle

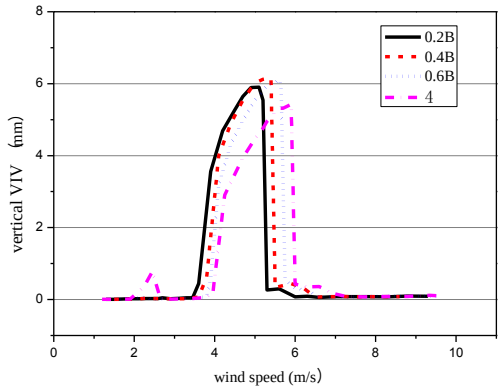

(e) uniform flow field，-3° wind attack angle

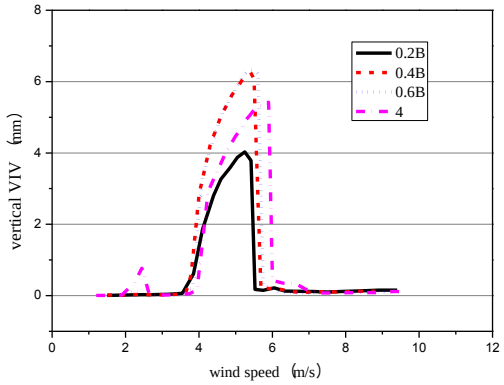

(f) turbulent flow field，-3° wind attack angle

Fig. 14 Responses of vertical VIV under two kinds of flow field, different wind attack angles and different heights from the ground

Section model test results of vertical VIV displacements are shown in Fig. 14:

(1) In the uniform flow field, ground effects do not change the width of VIV lock-in range, but impel vortex-induced vibrations to occur earlier, with wind speed intervals shift forward about 1m/s. This indicates that ground effects will speed up vortex shedding, thus making the VIV occur in advance. This conclusion is in accordance with that mentioned in section 3.4.

(2) In the turbulent flow field, since VIV is more sensitive to turbulence, lower height from the ground means higher turbulence so that vibration amplitude is reduced and vortex-induced vibration lock-in range is narrowed.

(3) Ground effects on VIV amplitudes vary at different wind attack angles. At the wind attack angle of +3°, ground effects reduce VIV amplitudes. In the case of -3°, ground effects have little impact on VIV amplitudes. At the wind attack angle of 0°, ground effects slightly increase the amplitude, but the impact is not significant.

(4) Comparing the results in both flow fields, it is found that under the same wind attack angle, the VIV lock-in ranges, as well as the amplitudes, are almost the same in two cases, which are H=0.6B and H=4.0B. It can be inferred from this phenomenon that when the height from the ground is over a certain value, ground roughness has little effect on VIV.

5. Ground effects on flutter stability

Fig. 15 presents torsional damping ratio variation curves of the closed box girder in four different heights from the ground, three different wind attack angles and two flow fields (uniform flow field and turbulence flow field). Fig. 16 gives the flutter critical wind speed test results under two kinds of flow field. Fig. 15 and Fig. 16 reveal that ground effects have a significant impact on flutter critical wind speeds of the closed box girder:

(1) In the uniform flow field, there is an approximate linear relationship between the height from ground and the flutter critical wind speed, but these do not appear in the turbulent flow field due to the complexity of turbulence.

(2) In the uniform flow field, flutter critical wind speeds dramatically reduce when the height from ground is reduced. In the case H/B=0.2, flutter critical wind speed has a reduction of 21.6%, 16.3% and 22.2% respectively, at wind attack angles of +3°, 0° and -3°. When H/B= 0.6, flutter critical wind speed has a reduction of 10.4%, 7.0% and 10.1% separately, at wind attack angles of +3°, 0° and -3°. This shows that reduced roughness has a dramatic negative influence on the flutter stability of the closed box girder.

(3) In the turbulent flow field, flutter critical wind speed of the closed box girder increases when the height from ground reduces at wind attack angle of +3°. Ground effects have a favorable impact on the stability of flutter, largely due to turbulence intensity. At wind attack angles of -3° and 0°, with the maximum reduction amplitude of about 5.9% and 7.1% individually, flutter critical wind speed reduces when the height from ground reduces, In other words, although the critical speed generally rises with respect to the increase in height from the ground, in most cases, the flutter critical speeds are still lower than those without consideration of ground effects. Ground effects adversely affect the flutter stability.

(4) In summary, regardless of the surface roughness, ground effects will adversely affect the flutter stability of the closed box girder. Ground effects should be fully considered during wind tunnel tests and engineering design.

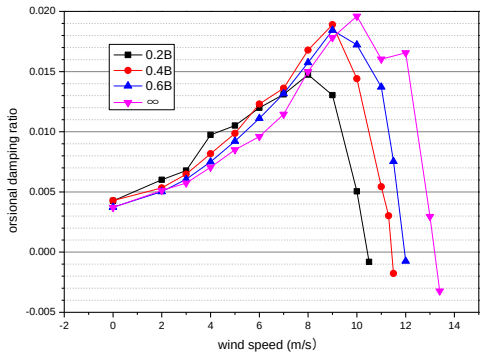

(a) uniform flow field，+3° wind attack angle

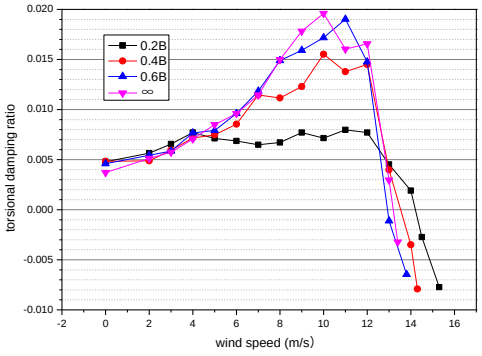

(b) turbulent flow field，+3° wind attack angle

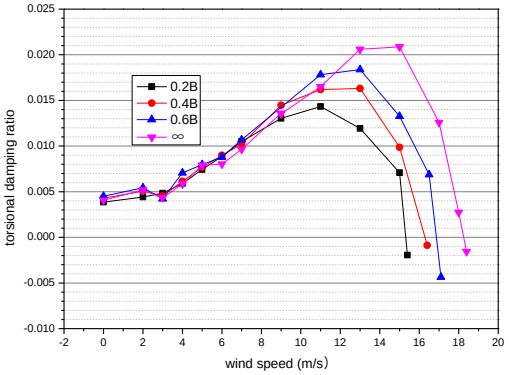

(c) uniform flow field，0° wind attack angle

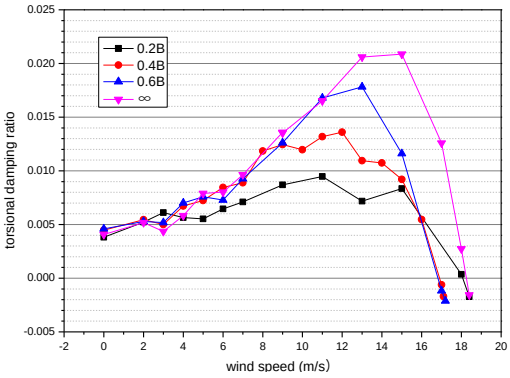

(d) turbulent flow field，0° wind attack angle

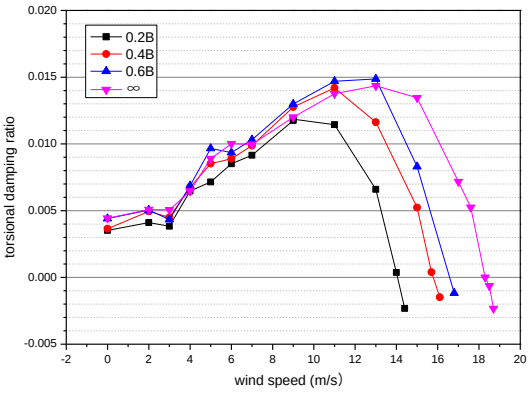

(e) uniform flow field，-3° wind attack angle

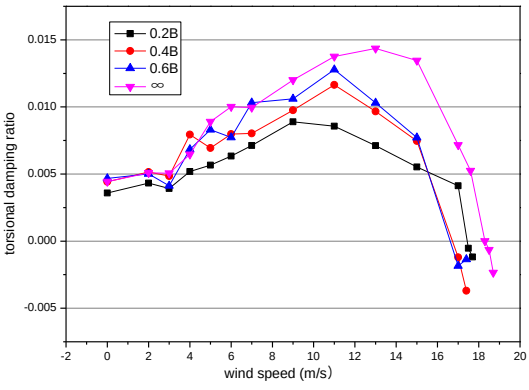

(f) turbulent flow field，-3° wind attack angle

Fig. 15 Torsional damping ratio curves under two kinds of flow fields, different wind attack angles and different heights from the ground

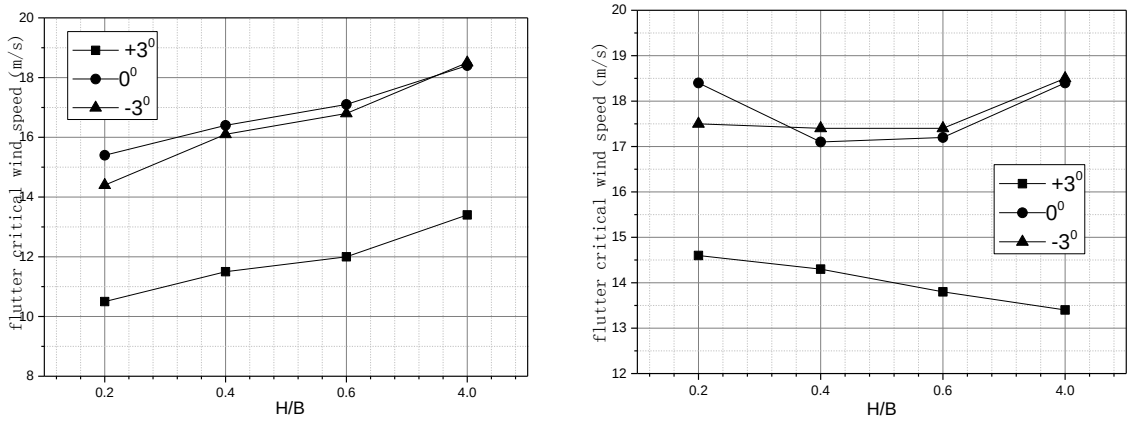

(a) uniform flow field (b) turbulent flow field

Fig. 16 The flutter critical wind speed test results

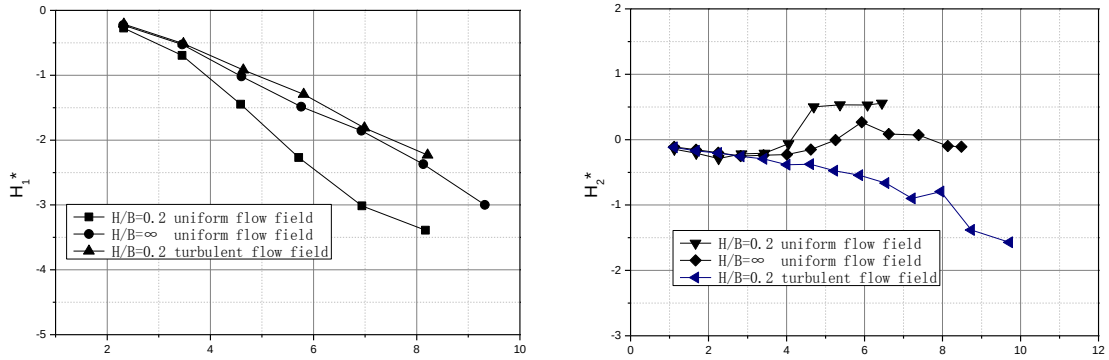

(a) The test value of the aerodynamic derivative H^*_1 (b) The test value of the aerodynamic derivative H^*_2

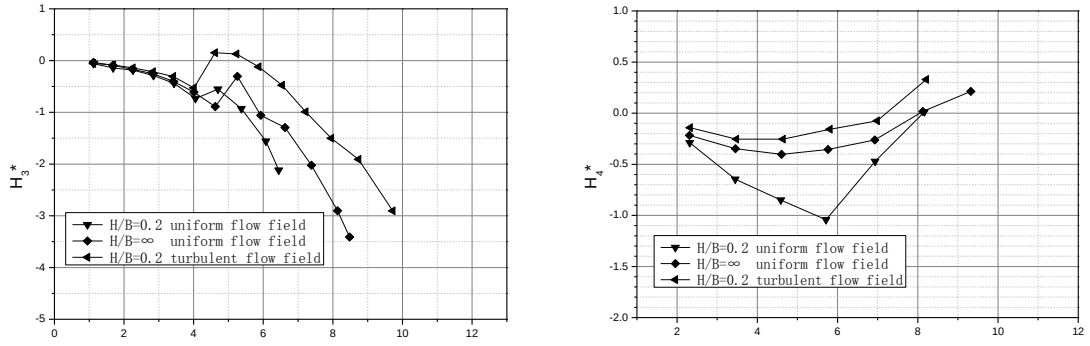

(c) The test value of the aerodynamic derivative H^*_3 (d) The test value of the aerodynamic derivative H^*_4

Continued-

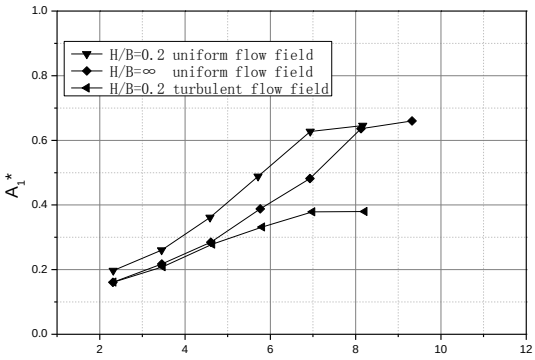

(e) The test value of the aerodynamic derivative A^*_1

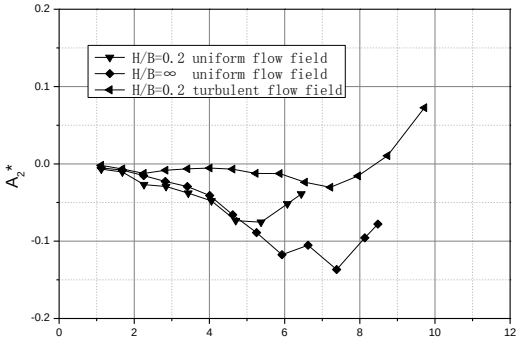

(f) The test value of the aerodynamic derivative A^*_2

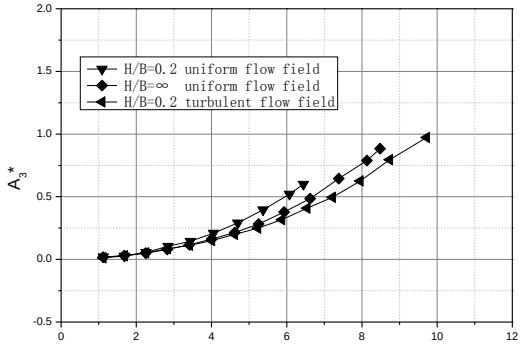

(g) The test value of the aerodynamic derivative A^*_3

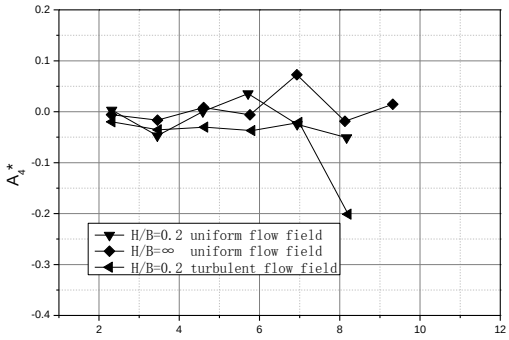

(h) The test value of the aerodynamic derivative A^*_4

Fig. 17 The aerodynamic derivative test values

Fig. 17 provides the aerodynamic derivative variation curves in this study. A^*_2 is an important parameter in flutter analysis that we can use it to preliminarily assess the flutter stability of structures. From Fig. 17(f)), A^*_2 shows a tendency from negative to positive and ground effects make this tendency occur in advance. This means that ground effects adversely affect the flutter stability.

6. Conclusions

Based on wind tunnel test method, ground effects on the aerodynamic force coefficients, the vortex-induced vibrations and the flutter stability of the closed box girder were studied in this paper. The main conclusions are summarized as follows:

(1) For the aerodynamic force coefficients, when the deck is getting closer to the ground, greater forces will be exerted on the deck. Ground effects will have a negative influence.

(2) For VIV, in the uniform flow field, without changing the width of VIV lock-in range, ground effects make VIV occur earlier by speeding up vortex shedding. In the turbulent flow field,

higher turbulence caused by ground effects reduces the vibration amplitude and narrows the lock-in range.

(3) When the height from the ground is over a certain value (about 0.4~0.6B), VIV phenomena resemble each other in two flow fields, regardless of ground roughness.

(4) For the flutter stability, in the uniform flow field, the flutter critical wind speed dramatically decreases when the height from ground reduces. This trend appears the same in the turbulent flow field except at wind attack angle of +3°, only in which ground effects has a favorable impact on the stability of flutter. In other words, the flutter critical speeds are still lower than those without consideration of ground effects in most cases. Ground effects adversely affects the flutter stability.

To sum up, regardless of the surface roughness, ground effects will adversely affect the aerodynamic force coefficients, the vortex-induced vibrations and the flutter stability of the closed box girder. Ground effects should be fully considered during wind tunnel tests and engineering design.

References

Barber, T. (2006), "Aerodynamic ground effects: a case study of the integration of CFD and experiments", *Int.J. Vehicle Des.*, **40**(4), 299-316.

Chen, A. R . and Zhou, Z. Y. (2006), "On the mechanism of vertical stabilizer plates for improving aerodynamic stability of bridges", *Wind Struct.*, **9**(1), 59-74.

Diana, G., Rocchi, D., Argentini, T. and Muggiasca, S. (2010), "Aerodynamic instability of a bridge deck section model: linear and nonlinear approach to force modeling", *J. Wind Eng. Ind. Aerod.*, **98**(6-7), 363-374.

Gross, J. and Traub, L.W. (2012), "Experimental and theoretical investigation of ground effects at low reynolds numbers", *J. Aircraft*, **49**(2), 576-586.

JTG/T D60-01-2004 (2004), *Wind-resistent Design Specification for Highway Bridges*, China Communications Press, Beijing, China

Larsen, A. (2000), "Aerodynamics of the Tamoca Narrows Bridge-60 years later", *Struct. Eng. Int.*, Hongkong, 243-248.

Lee, J., Han, C.S. and Bae, C.H. (2010), "Influence of wing configurations on aerodynamic characteristics of wings in ground effects", *J. Aircraft*, **47**(3), 1030-1036.

Mahon, S and Zhang, X. (2005), "Computational analysis of pressure and wake characteristics of an aerofoil in ground effects" , *J. Fluid. Eng.*, **127**(2), 290-298.

Marshall, D.W., Newman, S.J. and Williams, C.B. (2010), "Boundary layer effects on a wing in ground effects", *Aircraft Eng. Aerosp. Technol.*, **82**(2), 99-107.

Matsumoto, M., Yoshizumi, F., Yabutani, T., Abe, K. and Nakajima, N. (1999), "Flutter stabilization and heaving-branch flutter", *J. Wind Eng. Ind. Aerod.*, **83**(3), 289-299.

Mokry, M. (2001), "Numerical simulation of aircraft trailing vortices interacting with ambient shear or ground", *J. Aircraft*, **38**(4), 636-643.

Park, K. and Lee, J. (2008), "Influence of endplate on aerodynamic characteristics of low-aspect-ratio wing in ground effects", *J. Mech. Sci. Technol.*, **22**(12), 2578-2589.

Prasad, R. (2014), "Computational modeling of wing in ground effects aerodynamics", Indian Institute of Technology, Gandhinagar.

Sarwar, M.W. and Ishihara, T. (2010), "Numerical study on suppression of vortex-induced vibrations of box girder bridge section by aerodynamic countermeasures", *J. Wind Eng. Ind. Aerod.*, **98**(12), 701-711.

Williamson, C.H.K. and Govardhan, R. (2004), "Vortex-induced vibrations", *Annu. Rev. Fluid Mech.*, **36**(1), 413-455.

Wu, T. and Kareem, A. (2013), "Vortex-induced vibration of bridge decks: Volterra series-based model", *J. Eng. Mech.*, **139**(2), 1831-1843.
Yang, M., Yang, W. and Yang, Z.G. (2015), "Wind tunnel test of groud viscous effects on wing aerodynamics", *Acta Aerodynamica Sinica*, **33**(1), 82-86.
Yang, W. and Yang, Z.G. (2014), "Aerodynamic investigation on design of tiltable end plate flow wingcraft", *Aircraft Eng. Aeros.*, **84**(1), 4-12.
Yang, Y.X. and Ge, Y.J. (2009), "Aerodynamic flutter control for typical girder sections of long-span cable-supported bridges" , *Wind Struct.*, **12**(3), 205-217.
Zhou, Z., Yang, T., Ding, Q. and Ge, Y. (2015), "Mechanism on suppression in vortex-induced vibration of bridge deck with long projecting slab with countermeasures", *Wind Struct.*, **20**(5), 643-660.

AD